Analytical Biochemistry 433 (2013) 210–217

Contents lists available at SciVerse ScienceDirect

Analytical Biochemistry

journal homepage: www.elsevier.com/locate/yabio

An acrylamide biosensor based on immobilization of hemoglobin onto multiwalled carbon nanotube/copper nanoparticles/polyaniline hybrid film

Bhawna Batra, Suman Lata, Madhu Sharma, C.S. Pundir *

Department of Biochemistry, M.D. (Maharshi Dayanand) University, Rohtak 124001, India

ARTICLE INFO

Article history:
Received 13 August 2012
Received in revised form 15 October 2012
Accepted 18 October 2012
Available online 24 October 2012

Keywords:
Acrylamide
Hemoglobin
Copper nanoparticles
Carbon nanotubes
Polyaniline

ABSTRACT

A method is described for the construction of a highly sensitive electrochemical biosensor for the detection of acrylamide, based on covalent immobilization of hemoglobin (Hb) onto carboxylated multiwalled carbon nanotube/copper nanoparticle/polyaniline (c-MWCNT/CuNP/PANI) composite electrodeposited onto pencil graphite (PG) electrode. The enzyme electrode was characterized by cyclic voltammetry (CV), scanning electron microscopy (SEM), X-ray diffraction (XRD), transmission electron microscopy (TEM), Fourier transform infrared (FTIR) spectroscopy, and electrochemical impedance spectroscopy (EIS). The biosensor showed an optimal response at pH 5.5 (0.1 M sodium acetate buffer) and 35 °C when operated at 20 mV s^{-1}. The biosensor exhibited low detection limit (0.2 nM) with high sensitivity (72.5 μA/nM/cm^2), fast response time (<2 s), and wide linear range (5 nM to 75 mM). Analytical recovery of added acrylamide was 95.40 to 97.56%. Within- and between-batch coefficients of variation were 2.35 and 4.50%, respectively. The enzyme electrode was used 120 times over a period of 100 days, when stored at 4 °C.

Acrylamide is shown to be a neurotoxicant, a reproductive toxicant, and a carcinogen in animals [1]. Acrylamide is formed in the reaction between reducing sugars such as glucose and asparagine. The Maillard reaction mechanism accounts for its formation in high-starch foods during cooking at high temperatures [2–4]. Very high amounts of this toxic compound have been found in potato chips, with levels up to 4 mg/kg [5]. Among analytical methods reported for determination of acrylamide levels, gas chromatography (GC)[1]–mass spectrometry (MS) [6], GC–tandem MS (MS/MS) [7], high-performance liquid chromatography (HPLC)–MS [8], and liquid chromatography (LC)–MS/MS [9,10] predominate. However, these methods are cumbersome and require expensive apparatus and time-consuming sample preparation. The growing demand for rapid and precise determination of acrylamide has stimulated the development of alternative methods for screening this neurotoxin and carcinogen. Only a few examples using various techniques for detection of this toxic compound exist. The biosensors offer great promise for detection of biomolecules with simplicity, rapidity, and high sensitivity. It is known that acrylamide can create adducts with hemoglobin (Hb) [11–13]. The idea behind the proposed sensor was based on the reaction of Hb with acrylamide, which leads to the creation of an Hb–acrylamide adduct that could alter the electroactivity of Hb. As a result, with an increase of Hb–acrylamide adduct concentration at the electrode surface, the current peak decreases. The decrease of current can be treated as the analytical signal and a base for very selective and sensitive biosensors for acrylamide determination. Hb (MW = 64,500) is an assembly of four globular protein subunits noncovalently bound to each other. Interactions between these subunits result in the allosteric properties of this protein. Each of the four subunits is composed of a protein chain tightly associated with a nonprotein heme group, which is located in crevices near the surface of the molecule. The four iron–heme prosthetic groups are responsible for electroactivity of Hb undergoing the reversible change from Fe(III) to Fe(II). Hb is prone to both reversible and irreversible modification; the sixth position of the iron can be spontaneously occupied by small ligands such as oxygen, CO, or CN^-. The N-terminal amino acid of the β-chain reacts spontaneously with glucose via an unstable Schiff's base to form ketoimine of fructose. The cysteine residues of the β-chains are highly reactive and react with –NO and other –SH blocking reagents [14]. Acrylamide and related conjugated vinyl compounds undergo Michael-type nucleophilic addition reactions of amino ($-NH_2$) and sulfhydryl (–SH) groups of amino acids, peptides, and proteins to their double

* Corresponding author. Fax: +91 126274640.
E-mail address: pundircs@rediffmail.com (C.S. Pundir).

[1] *Abbreviations used:* GC, gas chromatography; MS, mass spectrometry; MS/MS, tandem MS; Hb, hemoglobin; PANI, polyaniline; CNT, carbon nanotube; cMWCNT, carboxylated multiwalled carbon nanotube; CuNP, copper nanoparticle; PG, pencil graphite; Carrez I, potassium hexacyanoferrate(II) trihydrate; Carrez II, zinc sulfate heptahydrate; EDC, *N*-ethyl-*N*′-(3-dimethylaminopropyl) carbodiimide; NHS, *N*-hydroxysuccinimide; SEM, scanning electron microscopy; UV, ultraviolet; TEM, transmission electron microscopy; XRD, X-ray diffraction; FTIR, Fourier transform infrared; DW, distilled water; DPV, differential pulse voltammetry; DDAB, didodecyldimethylammonium bromide; CV, coefficient of variation.

0003-2697/$ - see front matter © 2012 Elsevier Inc. All rights reserved.
http://dx.doi.org/10.1016/j.ab.2012.10.026

bonds. Investigations have shown that acrylamide–Hb adducts are formed as a result of the reaction between the α-NH_2 group of the N-terminal valine of Hb and acrylamide [11,12]. Hence, Hb can serve as useful biomarker of human exposure to acrylamide. The adsorption of such biomolecules onto the surface of nanoparticles can retain their bioactivity due to biocompatibility of nanoparticles [15]. Among various metal nanoparticles copper nanoparticles have attracted considerable attention, because of their good biocompatibility and catalytic, optical, and electrical conducting properties, resulting in increased response current [16].

Polyaniline (PANI), a conducting polymer, is unique due to its relatively facile synthesis, conductivity, and environmental stability [17–19]. Carbon nanotubes (CNTs) have been proved as an advanced and ideal material for supporting nanosized metallic particles in electrodes. To the best of our knowledge, there has been no report on the application of metallic nanoparticles along with CNTs and conducting polymer for fabrication of an acrylamide biosensor that is expected to improve the analytical performance of a biosensor. Here we describe the construction of an improved amperometric acrylamide biosensor by immobilizing Hb onto carboxylated multiwalled carbon nanotube (cMWCNT)/copper nanoparticle (CuNP)/PANI composite electrodeposited onto pencil graphite (PG) electrode.

Materials and methods

Materials

Human Hb from Sigma–Aldrich, c-MWCNTs (functionalized MWCNTs) from Intelligent Materials (Panchkula, India), aniline, hexane, acrylamide, potassium hexacyanoferrate(II) trihydrate (Carrez I), acetic acid, zinc sulfate heptahydrate (Carrez II), *N*-ethyl-*N*′-(3-dimethylaminopropyl) carbodiimide (EDC), *N*-hydroxysuccinimide (NHS), and copper sulfate from SISCO Research Lab (Mumbai, India) were used.

Apparatus

A potentiostat/galvanostat (Autolab, AUT83785, Eco Chemie) with a three-electrode system was composed of a Pt wire as an auxiliary electrode, Ag/AgCl electrode as a reference electrode, and Hb/cMWCNT/CuNP/PANI modified PG electrode as a working electrode. Scanning electron microscopy (SEM) was performed with a Zeiss device (EV040), ultraviolet (UV) spectroscopy was performed with a Shimadzu device (160 A), transmission electron microscopy (TEM) was performed with a JEOL device (2100 F), X-ray diffraction (XRD) was performed with a diffractometer (122 Rigaku, D/Max2550, Tokyo, Japan), and Fourier transform infrared (FTIR) spectroscopy was performed with a Thermo Scientific device.

Construction of Hb/cMWCNT/CuNP/PANI/PG electrode

Preparation of CuNPs

CuNPs were prepared using the chemical reduction method [16]. NaOH (0.1 M, 10 ml) was added to a mixture of aqueous solutions of $CuSO_4$ (0.4 M, 100 ml) and ethylenediaminetetraacetic acid (EDTA, 0.1 M, 10 ml). $NaBH_4$ (0.3 M, 100 ml) was added to this mixture solution and heated to 60 °C. After stirring for 45 min, the product was washed three times with ethanol and acetone separately and finally dried in a vacuum drying oven.

TEM of CuNPs

The morphological characterization of the copper nanoparticles was done in a transmission electron microscope at J.N. (Jawaharlal Nehru) University (New Delhi, India).

Electrodeposition of c-MWCNT/CuNP/PANI onto PG electrode

The surface of PG electrode (2 cm × 2 mm) was polished manually by alumina slurry (diameter of 0.05 μm) with a polishing cloth, followed by thorough washing with double distilled water (DW), and then placed into ethanol, sonicated to remove adsorbed particles, and finally washed with DW three or four times. cMWCNTs (1.0 mg) were suspended in a 4-ml mixture of concentrated H_2SO_4 and HNO_3 in a 3:1 ratio and ultrasonicated for 3 to 4 h to get its finely dispersed black-colored solution. The dispersed cMWCNT solution (0.1 ml) was mixed into a mixture of 0.5 ml of 0.2 M EDC and 0.5 ml of 0.2 M NHS (pH adjusted to 6.0) and kept at room temperature for 1 h. Aniline (400 μl) was added to 25.0 ml of 1 M KCl and electropolymerized onto graphite electrode through cyclic voltammetry using a potentiostat/galvanostat by applying 20 successive polymerization cycles at –0.1 to 0.2 V. CuNP suspension (400 μl) and 1.0 ml of cMWCNT suspension were added into 25 ml of 1 M KCl to get the cMWCNT/CuNP mixture. Finally, electrodeposition of CuNPs and cMWCNTs onto the graphite electrode was carried out in an electrochemical cell system using a potentiostat/galvanostat by applying 20 polymerization cycles at –0.1 to 0.2 V. During the electrochemical polymerization, the surface of graphite rod became green gradually, indicating the deposition of cMWCNT/CuNP/PANI film on PG electrode (Fig. 1). The resulting cMWCNT/CuNP/PANI/PG electrode was washed thoroughly with DW to remove unbound matter and kept in a dry Petri plate at 4 °C.

Immobilization of Hb onto cMWCNT/CuNP/PANI/PG electrode

cMWCNT/CuNP/PANI/PG electrode was placed into 2 ml of dissolved Hb (1 mg/ml, 0.2 M sodium acetate buffer, pH 5.0) and kept overnight at room temperature for immobilization. The resulting electrode (Hb/cMWCNT/CuNP/PANI/PG) was washed three or four times with 0.2 M sodium acetate buffer (pH 5.0) and used as a working electrode and stored at 4 °C when not in use. This working electrode was characterized by SEM at different stages of its construction.

SEM

The SEM images of bare graphite electrode, cMWCNT/CuNP/PANI/PG electrode, and Hb/cMWCNT/CuNP/PANI/PG electrode were taken in a scanning electron microscope (Zeiss EV040) at J.N. University, New Delhi on a commercial basis.

DPV measurement and testing of acrylamide biosensor

Differential pulse voltammetry (DPV) of Hb/cMWCNT/CuNP/PANI/PG electrode was recorded in a potentiostat/galvanostat from 0.075 to 0.275 V versus Ag/AgCl as a reference electrode and Pt

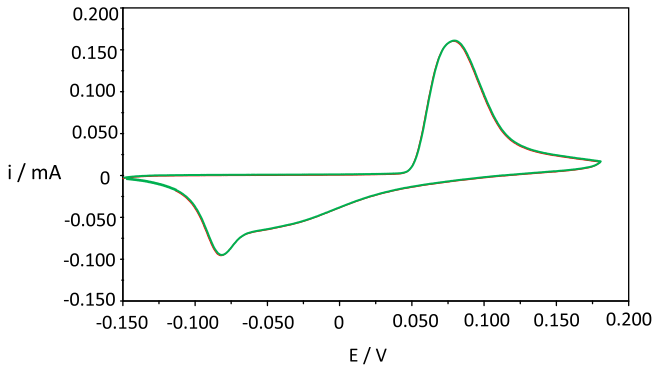

Fig.1. Cyclic voltammogram for electrodeposition of cMWCNT/CuNP/PANI composite film. Supporting electrolyte: 1 M KCl solution; Scan rate: 20 mV s^{-1}.

wire as a counter electrode in 30 ml of 0.2 M sodium acetate buffer (pH 5.5) containing 100 μl of 3.5 μM acrylamide.

Optimization of acrylamide biosensor

To optimize working conditions of the biosensor, the effects of pH, incubation temperature, time, and substrate (acrylamide) concentration on biosensor response were studied. To determine optimal pH, the pH of reaction buffer was varied between pHs 4.0 to 8.0 at an interval of 0.5 using the following buffers, each at a final concentration of 0.2 M: pHs 4.0 to 6.0, sodium acetate buffers; pHs 6.5 to 8.0, sodium phosphate buffers. Similarly, to determine the optimal temperature, the reaction mixture was incubated at temperatures ranging from 20 to 50 °C at an interval of 5 °C. The effect of acrylamide concentration on biosensor response was determined by varying the concentrations of acrylamide (in reaction mixture) in the range of 5 nM to 100 mM.

Application of acrylamide biosensor in potato crisp water extracts

Crushed potato crisps of different brands (4 g) were ground to powder pestle and mortar separately. The powder was added to DW (100 ml), and the sample was kept for 20 min to swell. The suspension was stirred for 1 h at 60 °C and then centrifuged at 4500 rpm for 20 min. The supernatant was collected and defatted by extraction with hexane. The obtained aqueous solution was purified by adding a mixture of 2.5 ml Carrez I (0.78 M) and Carrez II (0.5 M) in a 1:1 ratio. The upper aqueous solution was removed and filtered. Acrylamide content was measured in this filtrate by the current biosensor.

Storage stability of Hb/cMWCNT/CuNP/PANI/PG electrode

The stability of the working electrode was studied for 4 months by performing the assay on a weekly basis. It was stored in a dried condition at 4 °C when not in use.

Results and discussion

Characterization of CuNPs

The characterization of CuNPs was carried out by recording their UV and visible spectra with a UV–visible spectrophotometer (Fig. 2A), their TEM image with a transmission electron microscope (Fig. 2B), and their X-ray diffraction pattern with an X-ray diffractometer (Fig. 2C). UV and visible spectra exhibited a strong absorbance peak at 580 nm, confirming the synthesis of CuNPs (Fig. 2A). The typical TEM image of CuNPs (Fig. 2B) showed their spherical shape with an average size of 10 nm. The XRD patterns of the CuNPs clearly showed the characteristic peaks of CuNPs at 36.32°, 43.20°, and 50.32° (Fig. 2C).

SEM studies of PG electrode during its modification

The SEM images of the surface of bare PG electrode, cMWCNT/CuNP/PANI/PG electrode, and Hb/cMWCNT/CuNP/PANI/PG electrode are shown in Fig. 3A–C, respectively. The stepwise modification of electrode can be seen clearly from these SEM images. The SEM image of the bare PG electrode showed a smooth and featureless morphology (Fig. 3A). The cMWCNT/CuNP/PANI/PG composite film exhibited a net structure. Film is more uniform and porous (Fig. 3B); hence, the effective surface area is larger. On immobilization of Hb, the globular structural morphology appears due to attachment of Hb onto cMWCNT/CuNP/PANI/PG electrode (Fig. 3C).

Construction of acrylamide biosensor

Fig. 4 summarizes the construction of an acrylamide biosensor based on immobilization of Hb on CuNP decorated cMWCNTs and PANI composite film electrodeposited onto PG electrode. First, aniline was electropolymerized on the surface of PG electrode, because this method is easy and the layer thickness could be controlled, and then cMWCNTs and CuNPs were coelectrodeposited on the PANI coated PG electrode. To construct the working electrode, Hb was covalently immobilized onto cMWCNT/CuNP/PANI/PG electrode. Incubation of Hb solution with activated cMWCNT/CuNP/PANI/PG electrode leads to an effective collision between –COOH group of cMWCNT and $-NH_2$ groups on the surface of the Hb to form an amide (–CO–NH) bond through EDC and NHS chemistry. EDC and NHS activate the free –COOH groups of cMWCNT/CuNP/PANI composite layer. The differential pulse voltammograms of cMWCNT/CuNP/PANI/PG exhibited higher currents than PANI/PG, indicating that cMWCNT/CuNP/PANI/PG composite film has a larger effective surface area than PANI/PG composite film and that cMWCNT/CuNP/PANI/PG composite film could provide a conducting path through the composite matrix for faster kinetics. Hence, the cMWCNT/CuNPs, acting as electron transfer mediators, help in enhancing the biosensor response and, thus, increase its sensitivity. These observations also suggest that the cMWCNT/CuNP/PANI composite film provided a large surface area for immobilization of the Hb.

Response measurements of acrylamide biosensor

Acrylamide forms adducts with Hb as a result of the reaction between the $-NH_2$ group of the N-terminal valine of Hb. Formation of this adduct is associated with Hb structure change [4,5]. This structure change is probably responsible for the decrease of accessibility of redox-active centers of Hb immobilized on the surface of the electrode, which causes a decrease of current. Hb–acrylamide adducts altered the electroactivity of Hb and generated response of the biosensor. Investigated cMWCNT/CuNP/PANI/PG electrode modified with Hb displayed a quasi-reversible electrochemical reaction of Hb–Fe^{3+}/Hb–Fe^{2+}. The below mentioned scheme shows electrochemical reactions involved in electron communication on the surface of working electrode. The maximum response (current in mA) was observed at 0.194 V (Fig. 5); hence, subsequent studies were carried out at this voltage. This biosensor displayed electrochemical response toward the acrylamide with a linear range of 5 nM to 75 mM. As a consequence, in parallel with an increase of Hb–acrylamide adduct concentration at the electrode surface, the current peak of DPV decreases (Fig. 6). The results obtained show that a decrease of current can be treated as the analytical signal and could be a base for very selective and sensitive biosensors for acrylamide determination.

FTIR spectra

Fig. 7 shows FTIR spectra for PANI/Au electrode (panel A), cMWCNT/CuNP/PANI/PG electrode (panel B), and Hb/cMWCNT/CuNP/PANI/PG electrode (panel C). FTIR spectra of electrodeposited PANI/PG composite showed a band at 2925.17 cm^{-1} (Fig. 7A) due to N–H stretching of the benzenoid ring. The peak at 1560.52 cm^{-1} is assigned to the quinonoid ring, 1492.80 cm^{-1} is attributed to the benzoid ring, and 1115.02 cm^{-1} is attributed to the combination modes of benzenoid and quinonoid units. Fig. 7B shows the FTIR spectra of cMWCNT/CuNP/PANI/PG electrode, which showed several significant peaks. In the FTIR spectrum of Hb/cMWCNT/CuNP/PANI/PG bioelectrode (Fig. 7C), Hb binding is indicated by the appearance of additional bands at 1610 cm^{-1} assigned to the carbonyl stretch.

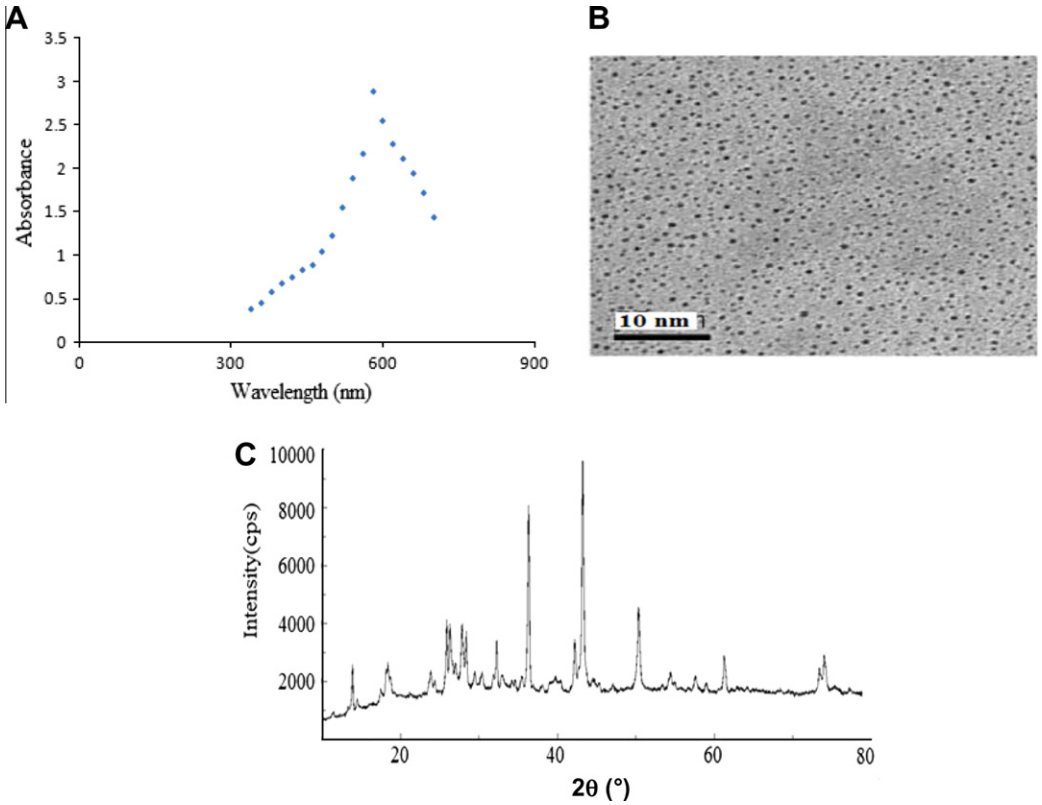

Fig.2. (A) UV–visible spectra of CuNPs. (B) TEM image of CuNPs. (C) XRD pattern of CuNPs.

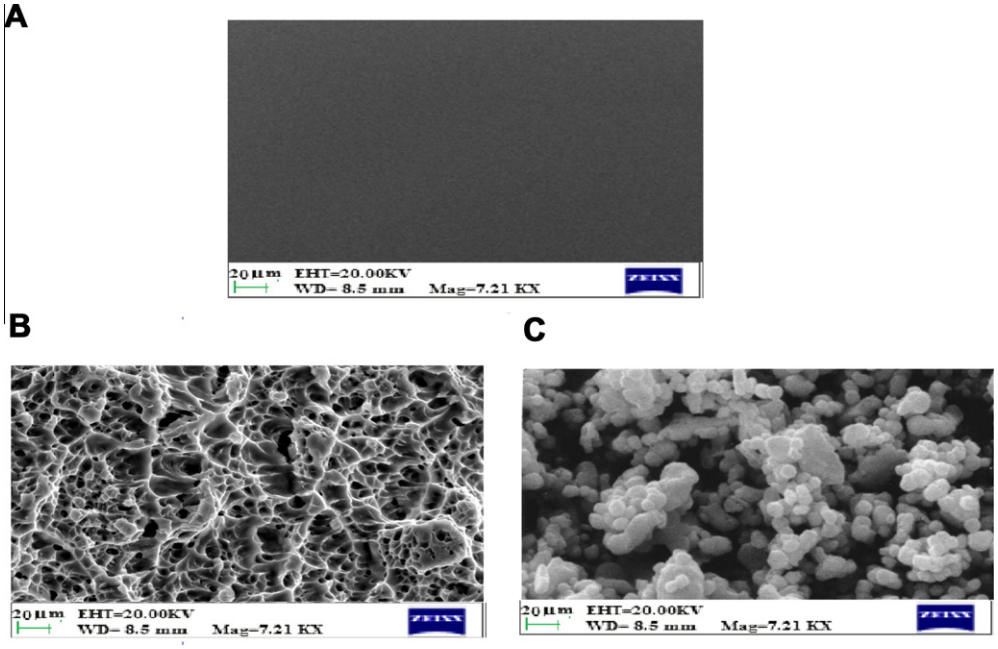

Fig.3. SEM images of bare PG electrode (A), cMWCNT/CuNP/PANI/PG (B), and Hb/cMWCNT/CuNP/PANI/PG electrode (C).

Electrochemical impedance measurements

Fig. 8 shows electrochemical impedance spectra of bare PG electrode (curve a), cMWCNT/CuNP/PANI/PG electrode (curve b), and Hb/cMWCNT/CuNP/PANI/PG electrode (curve c). The charge transfer process in Hb/cMWCNT/CuNP/PANI/PG electrode was studied by monitoring charge transfer resistance (R_{CT}) at the electrode and electrolyte interface. The value of the electron transfer resistance (semicircle diameter) (R_{CT}) depends on the dielectric and insulating features at the electrode/electrolyte interface. The R_{CT}

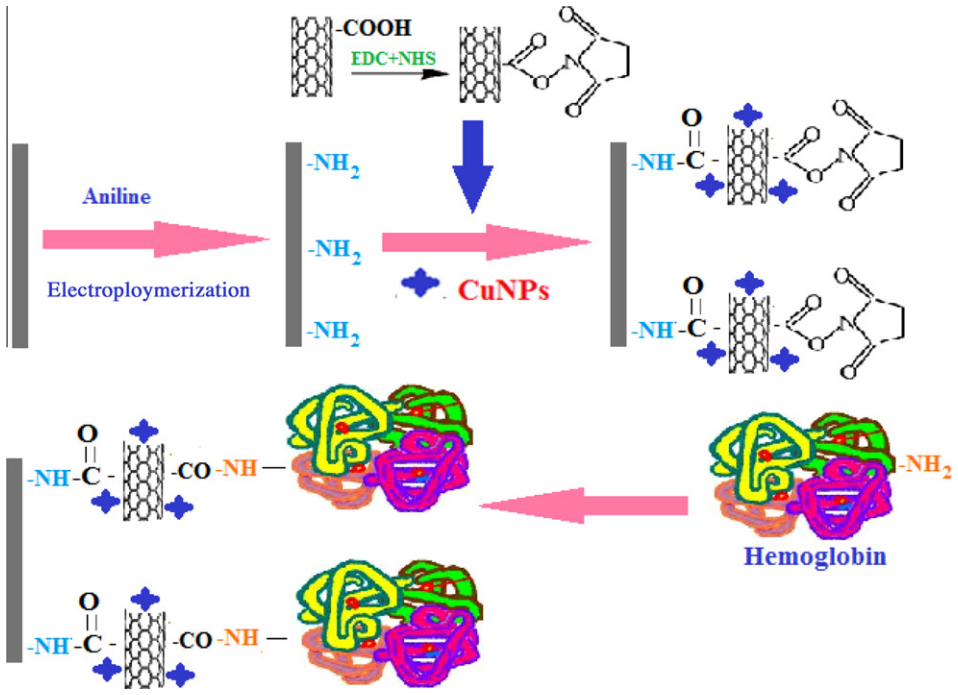

Fig.4. Schematic representation of chemical reaction involved in the fabrication of Hb/cMWCNT/CuNP/PANI/PG electrode.

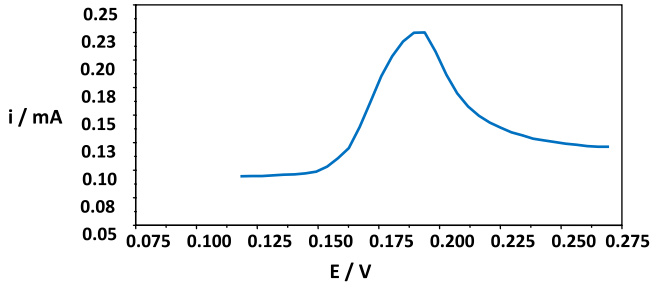

Fig.5. DPV response of Hb/cMWCNT/CuNP/PANI/PG on the addition of 100 µl (3.5 µM) acrylamide in 30 ml of 0.2 M sodium acetate buffer (pH 5.5) at various potentials at a scan rate of 20 mV s^{-1}.

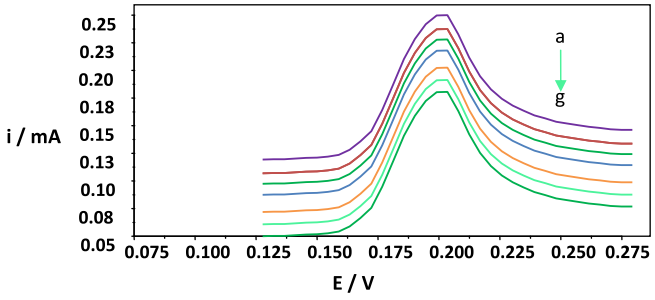

Fig.6. Differential pulse voltammogram measured with Hb/cMWCNT/CuNP/PANI/PG containing various concentrations of acrylamide in a solution with 0.2 M sodium acetate buffer (pH 5.5). Scan rate: 20 mV s^{-1}.

values for bare PG electrode, cMWCNT/CuNP/PANI/PG electrode, and Hb/cMWCNT/CuNP/PANI/PG electrode were 630, 580, and 400 Ω, respectively. This decreased R_{CT} value in the presence of Hb revealed that the electron transfer through redox couple was enhanced by the presence of Hb on the electrode surface.

Optimization of biosensor

The experimental conditions affecting the biosensor response were studied in terms of effect of pH, incubation temperature, time, and substrate (acrylamide) concentration. The optimal current was obtained at pH 5.5 (Fig. 9), which is almost similar to that of biosensor based on Hb–didodecyldimethylammonium bromide (DDAB) modified carbon paste electrode (pH 4.8) [20] and biosensor based on glassy carbon electrodes modified with single-walled carbon nanotubes/Hb (pH 5.0) [13]. The optimal temperature of the sensor was 35 °C (Fig. 10). The current response decreased rapidly after 35 °C due to thermal inactivation of the protein. Hence, the subsequent experiments were performed at 30 °C. There was a hyperbolic relationship between sensor response and acrylamide concentration in the range of 5 nM to 100 mM, and the response was constant after 75 mM.

Evaluation of biosensor

Linearity

There was a linear relationship between the current (in mA) and the acrylamide concentration in the range of 5 nM to 75 mM (Fig. 11), which is a better linear range than those of earlier biosensor based on Hb–DDAB modified carbon paste electrode (1.3×10^{-11} to 4.8×10^{-5} M) [20] and biosensor based on glassy carbon electrode modified with single-walled carbon nanotubes/Hb (1.0×10^{-11} to 1.0×10^{-3} M) [13].

Detection limit

The detection limit of the current sensor was 0.2 nM (signal/noise [S/N] = 3), which is lower than that of earlier biosensor based on glassy carbon electrode modified with single-walled carbon nanotubes/Hb (1.0×10^{-9} M) [13] but slightly higher than that of earlier biosensor based on Hb–DDAB modified carbon paste electrode (1.2×10^{-10} M) [20].

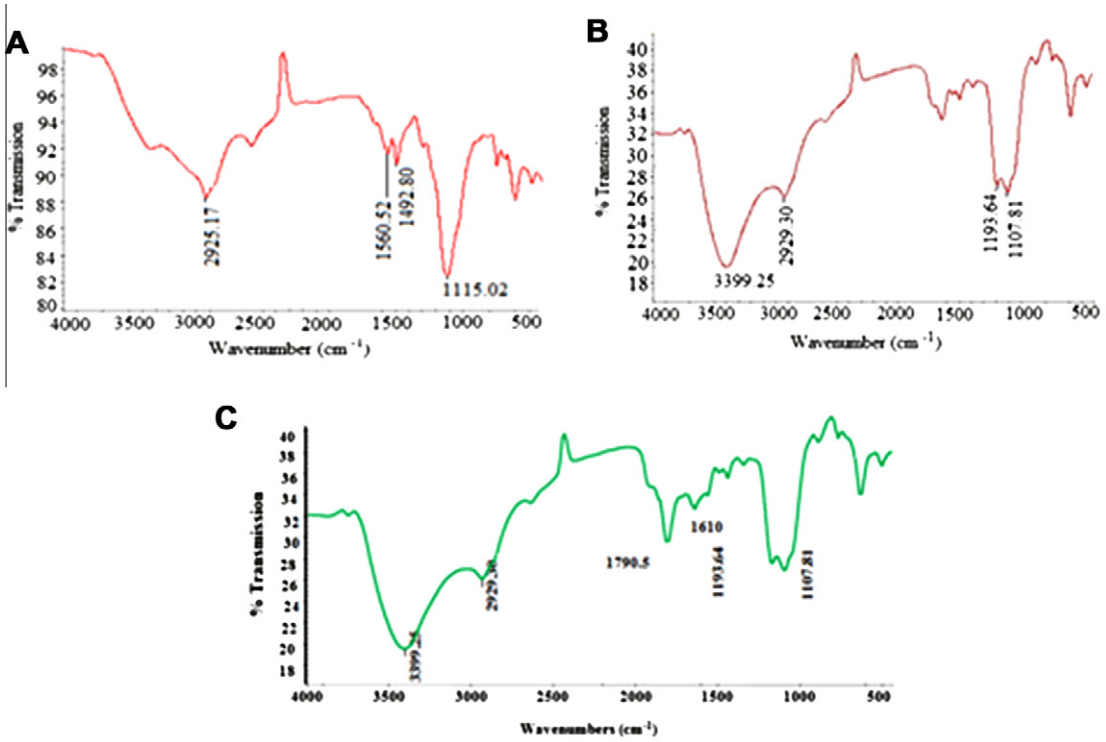

Fig.7. FTIR spectra of PANI/PG (A), cMWCNT/CuNP/PANI/PG (B), and Hb/cMWCNT/CuNP/PANI/PG (C).

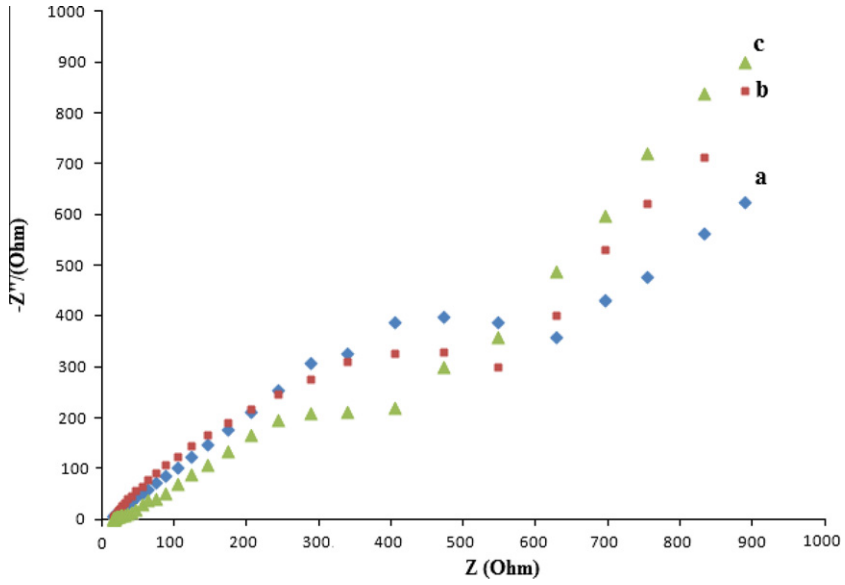

Fig.8. Impedance spectra of bare PG electrode (curve a), Hb/cMWCNT/CuNP/PANI/PG electrode (curve b), and cMWCNT/CuNP/PANI/PG electrode (curve c).

Analytical recovery

The average recoveries of acrylamide added to potato crisp water extract (at levels of 20 and 40 nM) varied from 95.40 to 97.56% (Table 1), demonstrating the satisfactory accuracy of the current biosensor.

Precision

Within- and between-sample coefficients of variation (CVs) for the determination of acrylamide in potato crisps on the same day and after 1 week of storage were 2.35 and 4.50%, respectively (Table 2). These high precisions highlight the good reproducibility and consistency of the current method, which can be attributed to the excellent immobilization of Hb onto the cMWCNT/CuNP/PANI/PG electrode.

Detection of acrylamide in potato crisps

Acrylamide levels as measured by the current biosensor ranged from 48.3 to 80.6 nM in potato crisps (Table 3). These values are comparable to those stated in earlier reports [13,20].

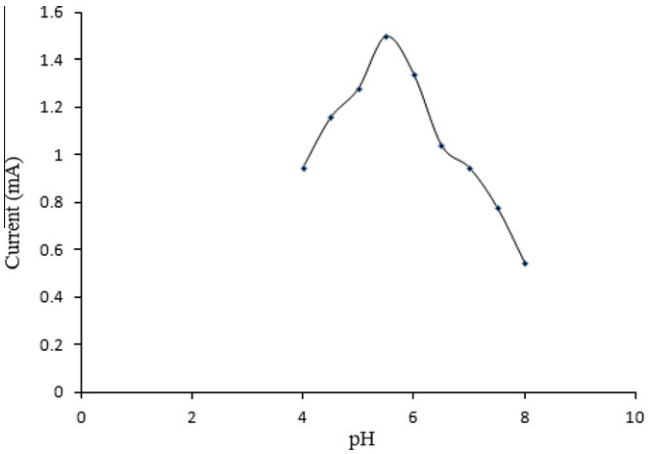

Fig.9. Effect of pH on Hb/cMWCNT/CuNP/PANI/PG electrode.

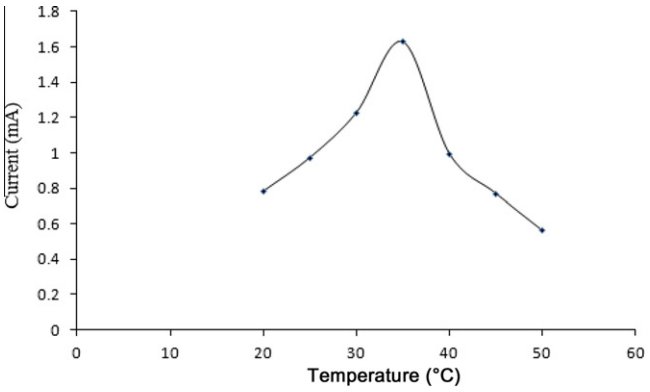

Fig.10. Effect of temperature on Hb/cMWCNT/CuNP/PANI/PG electrode.

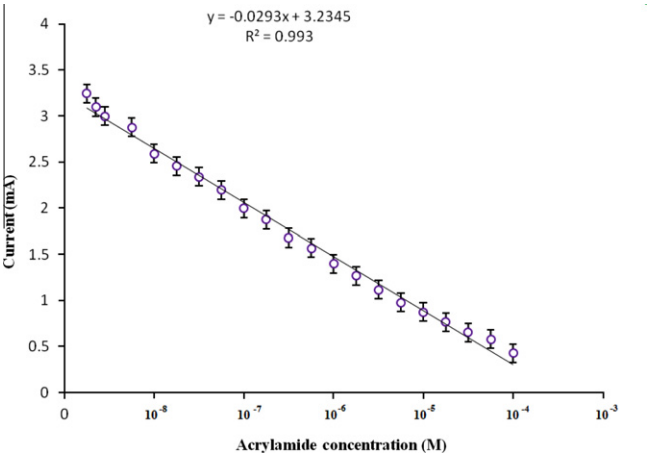

Fig.11. Hyperbolic curve for acrylamide biosensor for effect of acrylamide concentration on response of acrylamide biosensor based on cMWCNT/CuNP/PANI/PG electrode bound Hb.

Table 1
Analytical recovery of added acrylamide in potato crisps as measured by Hb/cMWCNT/CuNP/PANI/PG electrode.

Acrylamide added (nM)	Acrylamide found (nM)	% Recovery
–	12.50	100
20	31.90	95.40 ± 2.7
40	52.19	97.56 ± 3.1

Table 2
Within- and between-assay CVs for determination of acrylamide in potato crisps as measured by Hb/cMWCNT/CuNP/PANI/PG electrode.

n	Acrylamide (nM)	CV (%)
Within assay (6)		
70	72.16667	2.35
72		
75		
71		
73		
72		
Between assay (6)		
78	78	4.50
80		
80		
77		
80		
73		

Table 3
Acrylamide levels in various brands of potato crisps as measured by Hb/cMWCNT/CuNP/PANI/PG electrode.

Sample number	Brand name	Acrylamide concentration[a] (nM)
1	A	80.6 ± 0.3
2	B	72.9 ± 0.4
3	C	65.2 ± 0.2
4	D	48.3 ± 0.1

[a] Values are means ± standard deviations ($n = 4$).

Conclusion

An improved amperometric acrylamide biosensor was constructed by immobilization of Hb onto a hybrid of cMWCNTs and CuNPs attached onto PG electrode through conducting PANI film, which showed remarkably enhanced sensitivity and selectivity for acrylamide. The biosensor showed relatively rapid response, broad linear range, low detection limit (0.2 nM), good reproducibility, and long stability.

Acknowledgments

Bhawna Batra and Suman Lata are thankful to the Council of Scientific and Industrial Research (CSIR, India) for the awards of Junior and Senior Research Fellowships during this study.

References

[1] S.M. El-Assouli, Acrylamide in selected foods and genotoxicity of their extracts, J. Egypt. Public Health Assoc. 84 (2009) 371–390.
[2] D.S. Mottram, B.L. Wedzicha, A.T. Dodson, Food chemistry: acrylamide is formed in the Maillard reaction, Nature 419 (2002) 448–449.
[3] R.H. Stadler, L. Verzegnassi, N. Varga, M. Grigorov, A. Studer, S. Riediker, B. Schilter, Formation of vinylogous compounds in model Maillard reaction systems, Chem. Res. Toxicol. 16 (2003) 1242–1250.
[4] D.V. Zyzak, R.A. Sanders, M. Stojanovic, D.H. Tallmadge, B.L. Eberhart, D.K. Ewald, D.C. Gruber, T.R. Morsch, M.A. Strothers, G.P. Rizzi, M.D. Villagran, Acrylamide formation mechanisms in heated foods, J. Agric. Food Chem. 51 (2003) 4782–4787.
[5] B.E. Erickson, Finding acrylamide, Anal. Chem. 76 (2004) 247A–248A.
[6] M.M. Motaghi, M. Seyedain Ardebili, M. Honarvar, M. Mehrabani, A. Baghizadeh, Determination of acrylamide in selected types of Iranian breads by SPME technique, J. Food Biosci. Technol. 2 (2012) 57–64.
[7] L. Castle, S. Eriksson, Analytical methods used to measure acrylamide concentrations in foods, J. AOAC. Int. 88 (2005) 274–284.
[8] H. Ono, Y. Chuda, M. Ohnishi-Kameyama, H. Yada, M. Ishizaka, H. Kobayashi, M. Yoshida, Analysis of acrylamide by LC–MS/MS and GC–MS in processed Japanese foods, Food Addit. Contam. 20 (2003) 215–220.
[9] J. Rosén, K.E. Hellenäs, Analysis of acrylamide in cooked foods by liquid chromatography tandem mass spectrometry, Analyst 127 (2002) 880–882.

[10] W.C. Cheng, Y.M. Kao, D.Y.C. Shih, S.S. Chou, A.I. Yeh, Validation of an improved LC/MS/MS method for acrylamide analysis in foods, J. Food Drug Anal. 17 (2009) 190–197.
[11] E. Tareke, P. Rydberg, P. Karlsson, S. Eriksson, M. Tornqvist, Analysis of acrylamide, a carcinogen formed in heated foodstuffs, J. Agric. Food Chem. 50 (2002) 4998–5006.
[12] C. Ruden, Acrylamide and cancer risk: export risk assessments and the public debate, Food Chem. Toxicol. 42 (2004) 335–349.
[13] A. Stobiecka, H. Radecka, J. Radecki, Novel voltammetric biosensor for determining acrylamide in food samples, Biosens. Bioelectron. 22 (2007) 2165–2170.
[14] F.W. Scheller, N. Bistolas, S. Liu, M. Janchen, M. Katterle, U. Wollenberger, Thirty years of haemoglobin electrochemistry, Adv. Colloid Interf. Sci. 116 (2005) 111–120.
[15] X. Luo, A. Morrin, A.J. Killard, M.R. Smyth, Application of nanoparticles in electrochemical sensors and biosensors, Electroanalysis 18 (2006) 319–326.
[16] Q.L. Zhang, Z.M. Yang, B.J. Ding, X.Z. Lan, Y.J. Guo, Preparation of copper nanoparticles by chemical reduction method using potassium borohydride, Trans. Nonferrous Met. Soc. China 20 (2010) s240–s244.
[17] K.C. Persaud, P. Pelosi, in: J.W. Gardner, P.N. Bartlett (Eds.), Sensors and Sensory Systems for an Electronic Nose, Kluwer Academic, Boston, 1992, pp. 237–256.
[18] A.G. MacDiarmid, J.C. Chiang, M. Halpern, W.S. Huag, S. Mu, L.D. Somasiri, "Polyaniline": interconversion of metallic and insulating forms, Mol. Cryst. Liq. Cryst. 121 (1985) 173–180.
[19] T.A. Skotheim, R.L. Elsenbaumer, J.R. Reynolds, Handbook of Conducting Polymers, Marcel Dekker, New York, 1997.
[20] A. Krajewska, J. Radecki, H. Radecka, A voltammetric biosensor based on glassy carbon electrodes modified with single-walled carbon nanotubes/hemoglobin for detection of acrylamide in water extracts from potato crisps, Sensors 8 (2008) 5832–5844.